CATHODOLUMINESCENCE WAVELENGTH IMAGING STUDY OF CLUSTERING IN InAs/GaAs SELF-ASSEMBLED QUANTUM DOTS

D. H. RICH, C. ZHANG, I. MUKHAMETZHANOV, A. MADHUKAR
Department of Materials Science and Engineering, Photonic Materials and Devices Laboratory, University of Southern California, Los Angeles, California 90089-0241, danrich@usc.edu

ABSTRACT

Cathodoluminescence wavelength imaging (CLWI) of InAs/GaAs self-assembled quantum dots (SAQDs) was performed to study the spatial variation in the spectral lineshape of the broadened quantum dot (QD) ensemble. The lineshape was found to vary on a scale of ~μm, revealing attendant variations in the size distribution of SAQD clusters on this spatial scale. Energy variations in clusters of SAQDs are found to exhibit a spatial correlation with the efficiency of luminescence and the activation energy for thermal re-emission of carriers. A reduction in the energy variation of the QD clusters occurs when the thickness of the spacer layers in vertically self-organized samples is reduced or the number of stacks is increased. SAQDs were also prepared by punctuated island growth (PIG), in which deposition of the total desired amount is broken into two or more stages each separated by time delays. CLWI reveals a reduced variation in the energy of the dominant CL emission on a ~μm spatial scale, correlating with a narrower size distribution of larger QDs for PIG, as measured in atomic force microscopy.

INTRODUCTION

Scanning probe microscopy studies of the InAs island formation reveal the stochastic nature of the island formation, as the average size, variation in size, and distance between neighboring islands vary with coverage.[1] After growing a capping layer of GaAs, the InAs self-assembled quantum dots (SAQDs) form typically with a ~10% variation in size,[1] which leads to the characteristic 40-60 meV broadening of luminescence spectra in typical SAQD systems. The length scale on which the island size fluctuates is determined by the average inter-island separation distance, which ranges from 50 to 300 nm, and depends on the initial InAs coverage in the ~1.5 to 2.0 monolayer (ML) range.[1] Such fluctuations are evident in spatially resolved luminescence experiments which measure the discrete δ-like luminescence spectra of multi-excitonic transitions in isolated quantum dots (QDs).[2]

In this study, we employ cathodoluminescence wavelength imaging (CLWI) to enable a spatial mapping of the peak energy of the emission from the ensemble of QDs. We show that subtle variations in the SAQD lineshape for clusters on a scale of ~μm can be detected with CLWI. We have further explored the spatial correlation between the energy of interband transitions, CL luminescence efficiency, and the activation energy for thermal re-emission of carriers from the SAQDs on a μm-scale. We seek to better control the size distribution of QDs using a growth procedure called *punctuated island growth* (PIG).[3] This approach involves breaking the deposition of the total desired amount (θ_T) into two or more stages with the deposition in the first stage (θ_P) being in the well-formed 3D island regime. For InAs/GaAs(001), this corresponds to $\theta_T > 2$ ML and $\theta_P > 1.7$ ML. Atomic force microscopy (AFM) studies of QD samples grown with the PIG procedure demonstrate that the lateral growth (i.e., island base size) ceases at a critical base size.[3] The subsequent addition of InAs to such islands occurs through a change in the height of the islands, while maintaining a fixed self-limited base length. We have examined the effect of PIG on the CL lineshape and spatial variations in the energy of the primary CL peaks. We further

explore the relationship between the number of layers, interlayer spacing, and the magnitude of the QD peak energy variations in multi-layered vertically self-organized (VSO) samples.

EXPERIMENTAL

The SAQD samples were grown by MBE in which a total of 1.74 monolayers (ML) of InAs were deposited for each layer at a 500 °C substrate temperature and resulted in a lateral QD density of ~350 μm^{-2}. In the multi-layered VSO samples, 20- and 36-ML-thick GaAs spacers were grown at 400 °C by migration enhanced epitaxy (MEE) after each InAs deposition. The samples were capped with 170-ML MEE-grown GaAs. Details of the punctuated island growth procedure are discussed in Ref. 3. We have examined three samples grown with θ_T = 2.5 ML and θ_P = 1.74, 2.0 and 2.5 ML, the last of which is just the case for continuous 2.5 ML growth (i.e., a single stage growth). During the punctuated phase of the growth, the deposition is suspended for 60 s, after which the remaining InAs was deposited unitl the total coverage of 2.5 ML was reached. CL experiments were performed with a modified JEOL-840A scanning electron microscope (SEM).[4] A Ge p-i-n detector was used to detect the luminescence dispersed by a 0.25-m monochromator for CL imaging. CL spectroscopy was performed with an InGaAs linear array detector. CLWI is accomplished by acquiring a series of discrete monochromatic images, constructing a local spectrum at all 640 × 480 scan points within the image, and determining the wavelength, $\lambda_m(x,y)$, at which there is a peak in the CL spectrum at each scan point (x,y).

RESULTS AND DISCUSSION

We illustrate these results first with a stack plot of CL spectra acquired from a *two-layer* InAs sample whose spacer thickness is 36 ML. The 21 CL spectra in Fig. 1 are acquired locally along an arbitrary scan line of 57 μm in length by fixing the electron beam at each point, whose relative distance is indicated in the figure. The lineshape of each spectrum is observed to change at each position. The center of gravity of the spectral lineshape is roughly independent of the position. However, small changes in the lineshape give rise to a change in the peak position, λ_m. The spectra further appear to be composed of multiple components whose relative intensities change from one location to another. In further analysis, a dashed vertical line is marked at the point in each spectrum which has a maximum in intensity. It is therefore evident that the peak wavelength position, λ_m, varies along this line, owing to changes in the relative intensity of all components that comprise the spectra. Similar subtle variations in lineshape are observed for the single- and five-layer samples.

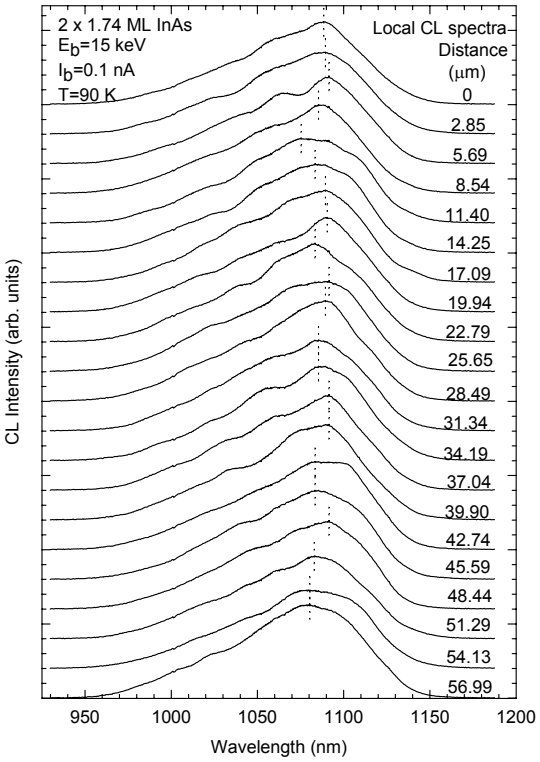

Figure 1. Stack plot of CL spectra acquired locally for an electron beam movement along an arbitray line of the two-layer SAQD sample.

Conventional monochromatic CL imaging reveals ~10% variation in the intensity of luminescence in the SAQD samples, with domain sizes on the order of a few microns, as shown in

Fig. 2(a) for the single layer sample (λ = 1050 nm). We estimate a spatial resolution of ~0.5 μm under the present CL imaging conditions. In order to examine spatial variations in λ_m, we have performed CLWI for four InAs SAQD samples composed of a single layer, two-layer with a 36 ML spacer, five-layer with a 36 ML spacer, and five-layer with a 20 ML spacer, as shown in Figs. 2 and 3. The samples were maintained at a temperature of 90 K. An electron beam of 15 keV and 1 nA was used to create the excess carriers in the samples. A false-color scale, with a color bar indicating the wavelength range, is shown for each image. Variations on a scale of ~μm in the peak wavelength position are observed in which domains of constant color are clearly visible. We observe the same type of variations and correlations in CLWI, independent of the position probed on each of the samples, which were ~5 mm x 5 mm in area.

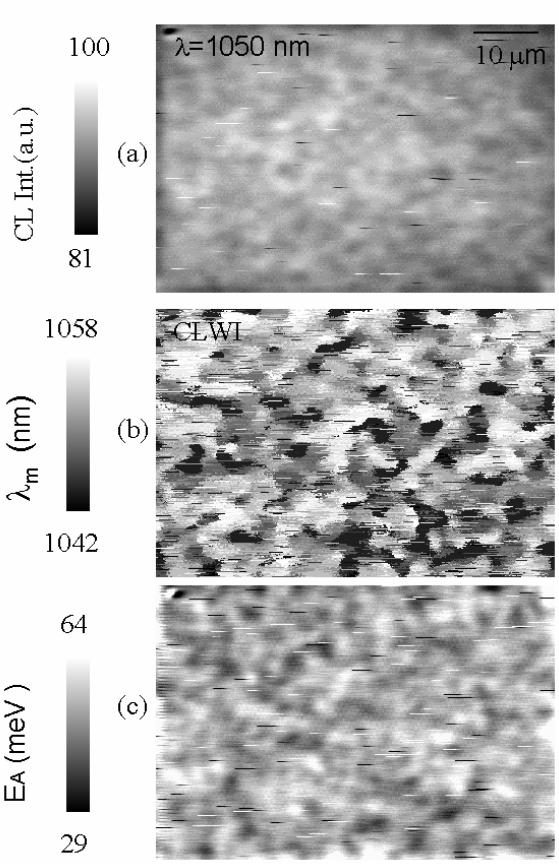

Figure 2. Monochromatic CL image (a), CLWI image (b) and activation energy image (c) for the single-layer QD sample.

In order to better understand such variations and their associated correlation, we have examined spatial variations in the temperature dependence of the luminescence. This is accomplished by recognizing that a thermally activated process is responsible for the reduction in the luminescence efficiency of the SAQDs as the temperature is increased. Previously, we have measured an activation energy associated with an Arrenhius behavior for SAQD samples.[5] In this analysis the logarithm of the CL intensity versus 1/T yields a nearly straight line from which a constant thermal activation energy, E_A, is obtained from the slope. We have extended this analysis to an imaging technique by determining E_A for all 640 x 480 points in a CL image by acquiring discrete monochromatic CL images in the 180 to 250 K range, thereby enabling a spatial mapping of E_A. Along with the monochromatic image, and CLWI image, we show an *activation energy image* in Fig. 2(c). The simultaneous acquisition of these three images for a fixed region of the sample enables an evaluation of the degree of spatial correlation of the associated optical properties measured.

An evaluation of the degree of correlation is illustrated by plotting the CL intensity, λ_m, and E_A versus distance along an arbitrary line, as shown in Fig. 4. The line scan analysis reveals a clear correlation between a red-shift in λ_m, an increase in E_A, and an increase in CL intensity, where peaks and dips in each of these three scans coincide. This correlation, while not perfect, illustrates a strong coupling in the optical behavior to the structural properties of the QDs on a μm-scale, which is the length scale on which these variations occur.

The intensity variations reflect size and shape dependent variations in the carrier capture into the QDs, spatial variations in thermally induced re-emission of carriers, and spatial variations in the density of localized defects, which can act as nonradiative recombination sites. On a scale of a few microns the images reveal a tendency for InAs QDs to form constant energy clusters, within the typical cation migration length of ~μm for In during MBE growth. The

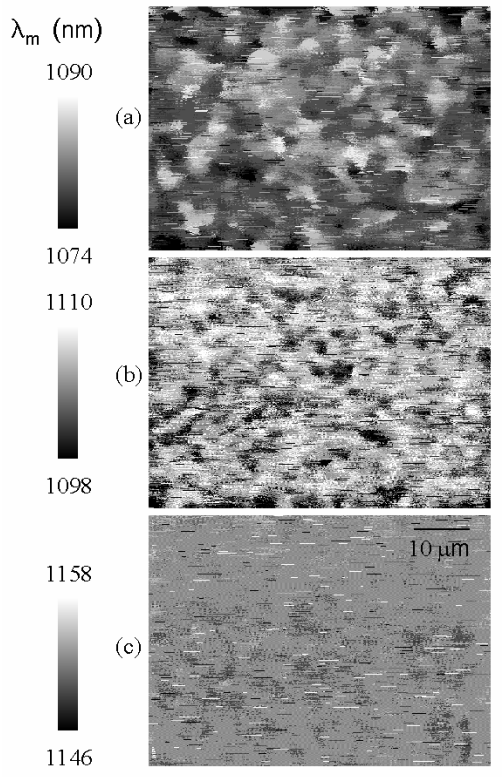

Figure 3. CLWI images of the two-layer with 36 ML spacer, five-layer with 36 ML spacer, and five-layer with 20 ML spacer samples in (a)-(c).

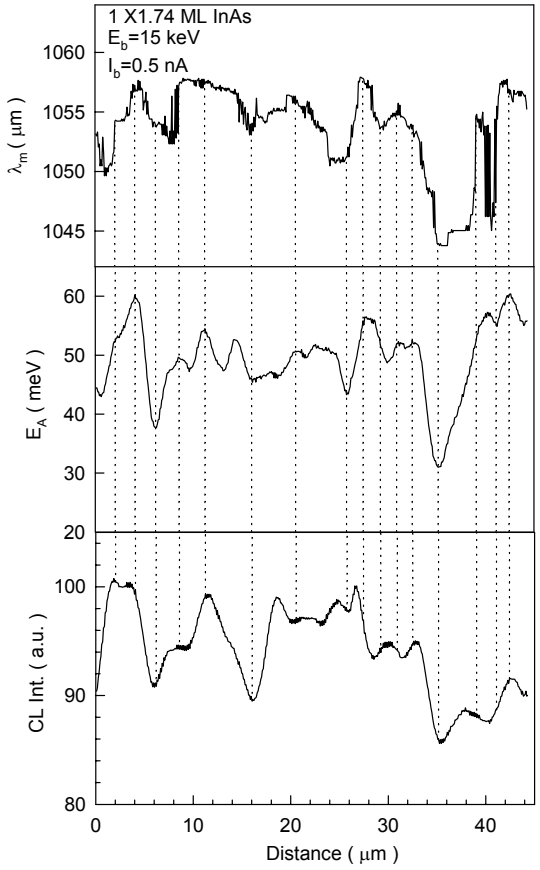

Figure 4. Line scan analysis of the single-layer sample showing the peak wavelength (λ_m), activation energy (E_A), and CL intensity versus distance along an arbitrary line. The vertical dashed lines illustrate the spatial correlation in peaks and dips for these scans.

strong corelation between peaks and valleys in λ_m, E_A, and intensity can be understood by a simple model, which connects the size of the QDs with the expected rates of thermal re-emission. Larger QDs, yielding a relative redshift in λ_m, also exhibit a larger confinement energy, owing to the larger energy separation between single particle electron and hole levels of the QDs and the single particle electron and hole levels of the wetting layer (WL). This in turn should lead to a larger E_A, which, in the limit of Boltzmann statistics, should represent the energy barrier for single particle excitation from confined QD levels to the WL levels. An E_A of ~40 to 50 meV is consistent with the energy difference between the QD and WL electron and hole levels, as determined by theoretical calculations[6] and previous estimates based on thermal quenching of the QD luminescence.[5] Finally, a larger barrier for thermal re-emission would also lead to a reduced re-emission rate, a larger steady-state carrier population in these larger QDs, and thus lead to a larger CL intensity, which is the third aspect of the correlation.

The domain size for the correlations in λ_m, E_A, and intensity are on the scale of a few microns. For an InAs delivery of 1.74 ML, the density of the SAQDs, as determined by a previous AFM measurement, is ~350 μm^{-2}.[1] We estimate that the blue- and red-shifted regions depicted in Figs. 2(b) and 3(a) represent regions containing ~300 to 3000 QDs. The energy shifts represent a subtle change in the size and shape distribution of QDs, as reflected by the change in weight of individual components that comprise a CL spectrum as the e-beam is moved from one domain to another (i.e., as in Fig. 1). The size scale of the domains is identical to the expected In

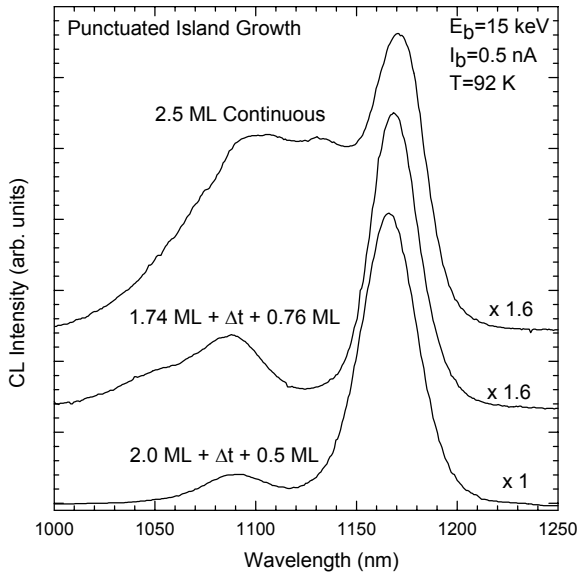

Figure 5. Local CL spectra excited with a fixed e-beam spot for QDs grown using the PIG approach**.**

cation migration length of ~1 μm for these growth conditions, thus allowing for the likelihood of small mass transfers from one domain to another during growth. The stochastic nature of self-assembly which leads to island size fluctuations on the 50 to 300 nm scale may likewise lead to fluctuations in the distributions of QD clusters on a ~1-10 μm scale, owing to the coverage-dependent size distribution of SAQDs and the likelihood for surface inhomogeneities to generate local variations in In diffusion and coverage. Such variations would then explain the observed *bimodal distribution* in the QD size fluctuations, where the first and second modes refer to the inter-island size variation and the inter-cluster size variations, respectively, on the 50-300 nm and 1-10 μm length scales. We note that a similar situation for a bimodal distribution in surface growth phenomena has been observed previously in the GaAs/AlGaAs quantum well (QW) system, where an atomic scale interface roughness is found to be superimposed upon a ~60 nm to ~1 μm variation in island size.[7]

We observe that the growth of five-layer samples resulted in marked changes in the spatial variation of λ_m, as seen in Figs. 3(b) and 3(c) for the 36 and 20 ML spacers, respectively. The standard deviations in the wavelength fluctuation ($\delta\lambda_m$) for the CLWI images of the single-layer, two-layer (36 ML spacer), five-layer (36 ML spacer), and five-layer (20 ML spacer) samples are 4.4, 3.2, 2.3, and 0.88 nm, respectively. The length scale of the fluctuations in λ_m and $\delta\lambda_m$ both decrease for the latter two VSO samples. This behavior is consistent with the improved uniformity that is expected to occur in the upper layers of VSO structures owing to the strain-driven In migration and subsequent formation of In island above buried islands. A further decrease in $\delta\lambda_m$ in going from the sample with a 36 ML spacer to the sample with a 20 ML spacer is due to the larger strain fields in the 20 ML spacer which enhance the QD size uniformity and is also possibly due to a larger inter-layer electronic coupling of QDs in samples with smaller spacer thicknesses. Photoluminescence of these structures shows a reduced line width relative to the single layer samples, consistent with the improved uniformity.[8] The average distance between centers of clusters is observed to decrease from ~5.0 to 2.5 μm in going from the single- and two-layer samples to the five-layer samples. The factor of ~2 reduction in the size scale of the clusters may reflect the presence of surface strain fields that reduce the effective cation migration length in the five-layer samples.

Local CL spectra of the samples grown using the PIG procedure are shown in Fig. 5. The wavelength position of the dominant peak (~1160-1175 nm) for each sample was again probed with CLWI, and the results are shown in Fig. 6. The total InAs deposition for each sample is θ_T = 2.5 ML and the depositions in the initial stage (θ_P) are 2.5, 1.74, and 2.0 ML for Figs. 6(a)-6(c), respectively. The wavelength fluctuation values ($\delta\lambda_m$) are, respectively, 0.72 , 0.67, and 0.30 nm for the samples in Figs. 6(a)-6(c). Like the single layer and VSO samples above, the 2.5 ML continuously grown and the 1.74 ML PIG sample exhibit the formation of domains of constant peak wavelength, λ_m, indicative of the formation of clusters whose mean separation is a few

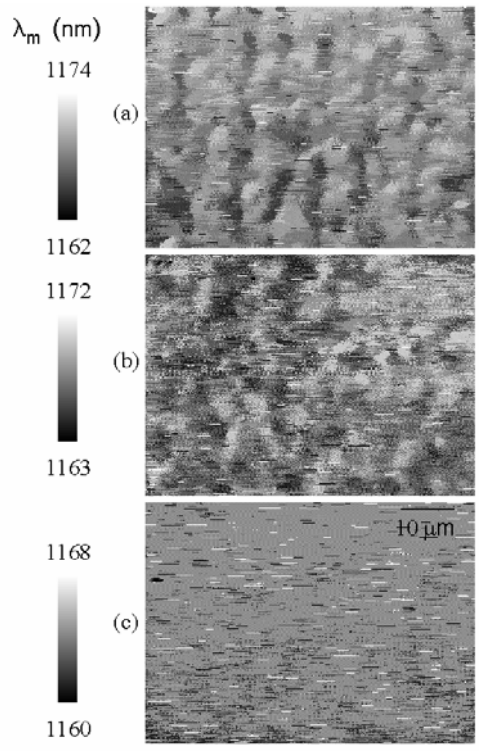

Figure 6. CLWI of PIG samples for θ_T = 2.5 ML. The samples were grown with θ_P = 2.5 ML (a), θ_P = 1.74 ML (b), and θ_P = 2.0 ML (c).

microns. When θ_P is 2.0 ML, however, the CLWI shows a marked reduction in the tendency for clustering on the ~μm scale. We hypothesize that the process of a self-limiting lateral base size is more complete during an initial phase deposition of 2.0 ML versus the case for 1.74 ML, and results in a reduced sensitivity to local variations in actual coverage that give rise to the clustering effects observed in the single-layer and VSO samples (Figs. 2 and 3, respectively).

The linewidths of the dominant CL peaks (1160-1175 nm) are 110, 25, and 29 meV, as shown in Fig. 5 for initial stage depositions of 2.5, 1.74 and 2.0 ML. The concomitant reduction in $\delta\lambda_m$ and linewidth for samples containing the latter two PIG stages of 0.76 and 0.5 ML is consistent with an increased uniformity and presence of large volume QDs. AFM studies of samples grown using PIG show that the InAs islands reach a self-limiting lateral size for a ~2 ML first stage deposition, after which, a subsequent deposition results primarily in an increase in the height of the islands.[3] The net increase in volume of the islands, following by MEE capping, has resulted in single binary InAs/GaAs QDs exhibiting the longest emission wavelength (~1250 nm) at low-temperatures and narrowest CL and photoluminescence[3] linewidths of ~25 meV.

In conclusion, we have observed a length scale of ~μm on which energy and intensity fluctuations occur for SAQDs. Energy variations in clusters of SAQDs are found to further exhibit a spatial correlation with the efficiency of luminescence and the activation energy for thermal re-emission of carriers. Multi-layered SAQD samples exhibit a reduction in the energy variations, owing to the stress-directed migration of In during growth. The CLWI results of the InAs/GaAs PIG samples here show further that the wavelength fluctuations on a ~μm spatial scale can be significantly reduced by choosing an initial deposition of 2 ML, followed by a 0.5 ML final deposition after the time delay.

This work was supported by AFOSR under the MURI FY '98 program.

REFERENCES

1. Q. Xie, N. P. Kobayashi, T. R. Ramachandran, A. Kalburge, P. Chen, and A. Madhukar, J. Vac. Sci. Technol. B **14**, 2203 (1996).
2. E. Dekel, D. Gershoni, E. Ehrenfreund, D. Spektor, J. M. Garcia, P. M. Petroff, Phys. Rev. Lett. **80**,4991 (1998).
3. I. Mukhametzhanov, Z. Wei, R. Heitz, and A. Madhukar, Appl. Phys. Lett. **75**, 85 (1999).
4. H. T. Lin, D. H. Rich, A. Konkar, P. Chen, and A. Madhukar, J. Appl. Phys. **81,** 3186 (1997).
5. Y. Tang, D. H. Rich, I. Mukhametzhanov, P. Chen, and A. Madhukar, J. Appl. Phys. **84**, 3342 (1998).
6. L.W. Wang, J. Kim, and A. Zunger, Phys. Rev. B**59,** 5678 (1999).
7. C. A. Warwick and R. F. Kopf, Appl. Phys. Lett. **60**, 386 (1992).
8. R. Heitz, A. Kalburge, Q. Xie, M. Grundmann, P. Chen, A. Hoffman, A. Madhukar, and D. Bimberg, Phys. Rev. B**57**, 9050 (1998).